Relativistic electric-dipole matrix-element zeros

L. A. LaJohn and R. H. Pratt
Department of Physics and Astronomy, University of Pittsburgh, Pittsburgh, Pennsylvania 15260
(Received 27 May 2002; published 11 March 2003)

There exists a class of relativistic electric-dipole matrix-element zeros which occur in $(n,l,j)\rightarrow(\epsilon,l+1,j)$ transitions at the photon energy $\omega^0=mc^2/(l+1)$, independent of the potential V as well as n and Z. These zeros do have observable physical consequences, despite the fact that they occur at high energies where multipole matrix elements are important.

DOI: 10.1103/PhysRevA.67.032701 PACS number(s): 32.80.Fb

I. INTRODUCTION

Matrix-element zeros in radiative transitions have been observed at energies of order mc^2 [1]. Here we report on electric-dipole matrix-element zeros that occur in this energy regime, which we will call relativistic dipole matrix-element zeros (RDZ's). RDZ's are fundamentally different from all other types of zeros. The position of these zeros with respect to photon energy ω is independent of the primary quantum number n, the atomic nuclear charge Z, the central potential V, and dipole retardation. The position ω^0 of RDZ's is determined entirely by the bound-state orbital angular momentum quantum number l_b, according to the simple formula $\omega^0=mc^2/(l_b+1)$ exactly. RDZ's occur only in $(n,l_b,j_b)\rightarrow(\epsilon,l_b+1,j_b)$ transitions, that is, when $\kappa_b<0$ and $|\kappa_b|=|\kappa_c|$ [κ is the relativistic Dirac equation quantum number defined as $\kappa=\mp(j+1/2)$ as $j=l\pm1/2$; the subscripts b and c correspond to the bound and continuum states, respectively]. The behavior of RDZ's is summarized in Table I. It should be noted that, although these are high energies, measurements of photoionization have already been performed in this range [2,3]. We will argue that it should be possible to observe the consequences of RDZ's.

RDZ's, unlike all other classes of zeros, are not influenced by any detailed atomic properties of the bound and continuum states, by n, Z, or V. We may briefly review these classes of zeros and their properties.

(1) *Low-energy zeros* that cause Cooper minima (CM), which exist in screened Coulomb potentials but not in point Coulomb potentials [4]. These are associated with the breaking of the Coulomb degeneracy in angular momentum in the presence of screening [5]. In the ground state, they occur in $(n,l_b)\rightarrow(\epsilon,l_b+1)$ dipole transitions in the nonrelativistic case. In the relativistic case [6] they occur in $(n,l_b,j_b)\rightarrow(\epsilon,l_c,j_c)$ transitions, where again $l_c=l_b+1$, with (i) $j_b=l_b-1/2$ and $j_c=l_b+1/2$, (ii) $j_b=l_b+1/2$ and $j_c=l_b+1/2$, and (iii) $j_b=l_b+1/2$ and $j_c=l_b+3/2$. In excited-state atoms multipole zeros are possible and they can also occur in $l_b\rightarrow l_b-1$ transitions [5]. Such zeros also occur in higher-multipole matrix elements [7]. These zeros, unlike RDZ's, are strongly dependent on n, l, and Z and occur at near-threshold energies.

(2) *Ultrahigh-Z low-energy point Coulomb relativistic zeros*, associated with the breaking of degeneracy in l for a given j in hydrogen [8]. At above-threshold energies, they occur in $ns_{1/2}\rightarrow\epsilon p_{3/2}$ transitions when $Z\geqslant128$ and in $np_{1/2}\rightarrow\epsilon d_{3/2}$ transitions when $Z\geqslant133$ [8]. Unlike RDZ's, they occur at near-threshold energies and only in $j\rightarrow j+1$ transitions (rather than in $j\rightarrow j$ transitions as in the case of RDZ's).

(3) *Higher-energy nonrelativistic Coulomb zeros* only occur in nondipole matrix elements at photon energies ranging from 1 to about 50 keV. In the quadrupole case they only occur in $(n,l_b)\rightarrow(\epsilon,l_c)$ transitions in which $l_c=l_b+2$ [5,9]. These zeros, present in a Coulomb potential, generally occur at high enough energies that they are largely independent of electron screening. Like low-energy CM, they can strongly affect angular distributions. These three classes of zeros, unlike RDZ's, show at least some dependence on n, Z, and V and have a more complicated dependence on l_b.

(4) *High-energy relativistic multipole zeros*. In addition to the RDZ's we are discussing here, we have also observed nondipole relativistic zeros which occur at energies of order mc^2. Unlike RDZ's they show dependences on n and Z that range from nearly independent to strongly dependent, with more complicated dependence on l_b. Unlike RDZ's, it is not clear whether these higher-multipole zeros have physical consequences, in photoionization or in related processes.

Despite the fact that RDZ's occur at energies for which nondipole effects matter, they still have observable physical consequences. The most striking effect occurs in the photon-electron polarization correlation coefficient C_{23}. This coefficient gives the correlation between longitudinal polarization of electrons produced by photoionization and the linear polarization of the incident photons out of the production plane. C_{23}, like the other six nonzero C_{ij}'s, are physically observable quantities that can be measured. For example, C_{10} has been measured for elements such as Pt, Pb, Ta, Au, and U at energies in the MeV range [2] and C_{02} was measured for Au at 662 keV [3].

TABLE I. Summary of RDZ behavior.

Transition	κ_b	κ_c	l_b	ω^0 (units of mc^2)	ω^0 (keV)
$ns_{1/2}\rightarrow\epsilon p_{1/2}$	-1	1	0	1	511
$np_{3/2}\rightarrow\epsilon d_{3/2}$	-2	2	1	1/2	255.5
$nd_{5/2}\rightarrow\epsilon f_{5/2}$	-3	3	2	1/3	170.3
$nf_{7/2}\rightarrow\epsilon g_{7/2}$	-4	4	3	1/4	127.75

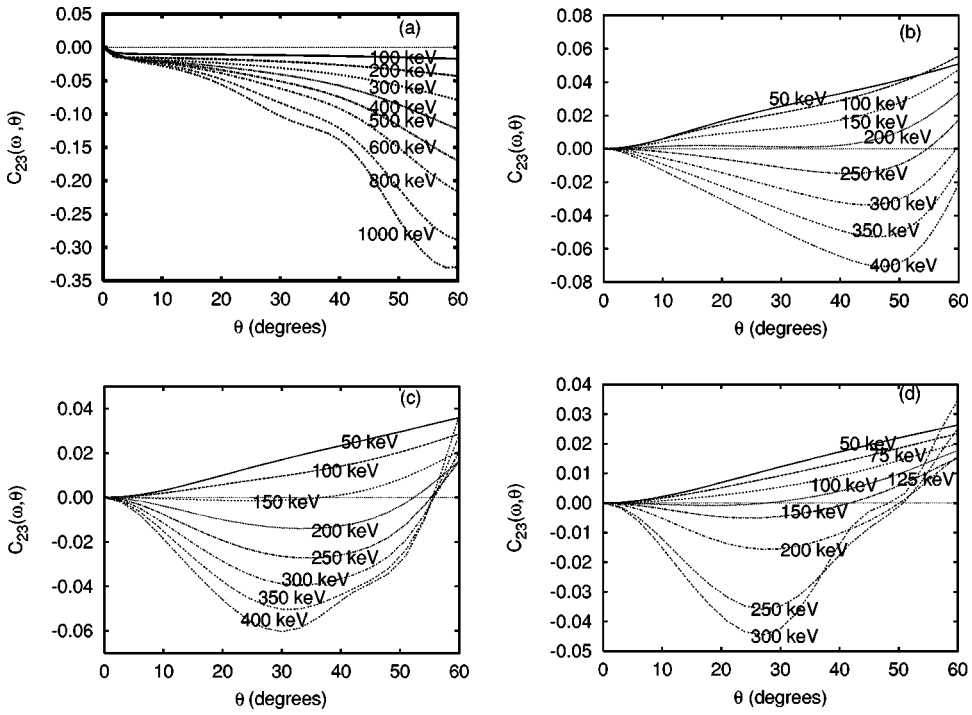

FIG. 1. Photon-electron polarization coefficient C_{23} [see Eq. (2)] for photoionization of neodymium ($Z=60$):
(a) $4s_{1/2}$, $\omega^0=511$ keV;
(b) $4p_{3/2}$, $\omega^0=255.5$ keV;
(c) $4d_{5/2}$, $\omega^0=170.3$ keV;
(d) $4f_{7/2}$, $\omega^0=127.75$ keV.
The calculation is fully relativistic within the independent-particle approximation using the Dirac-Slater potential. The first ten electric- and magnetic-field matrix elements are included in all calculations.

The full differential cross section including polarization may be written as

$$\frac{d\sigma}{d\Omega}(\omega,\theta,\phi)=\frac{1}{2}\left[\frac{d\sigma}{d\Omega}\right]_{\text{unpol}}(\omega,\theta)\sum_{ij}\xi_i\chi_j C_{ij}(\omega,\theta), \quad (1)$$

where C_{ij} are the photon-electron polarization coefficients. All C_{ij} values are on a scale of unity with the unpolarized contribution $C_{00}=1$. Here θ is the angle between the ejected electron and the incident photon direction (z axis); the ξ_i are the Stokes parameters describing photon polarization; χ_j are the components of the unit vector for the spin direction of the electron in its rest system [10,11] ($\xi_0=\chi_0=1$). Also $[d\sigma/d\Omega]_{\text{unpol}}=(\sigma/2\pi)S(\omega,\theta)$, with σ the total cross section, $S(\omega,\theta)=\Sigma_l B_l P_l(\cos\theta)$, where B_l and P_l are the angular distribution parameters and the Legendre polynomials, respectively [8–10]. Note that, from general considerations, the differential cross section (1) is bilinear in the electron spin and the Stokes parameters ξ_i, and C_{ij} only depends on $\hat{\mathbf{p}}\cdot\hat{\mathbf{k}}$. Thus if the coordinate is chosen [see Fig. 2 in [10]] such that the z axis is along $\hat{\mathbf{k}}$ and the y axis along $\hat{\mathbf{k}}\times\hat{\mathbf{p}}$, then the angle $\hat{\mathbf{p}}\cdot\hat{\mathbf{k}}$ is the polar angle, as indicated, and the azimuthal angle ϕ only enters in the Stokes and spin parameters, not in $C_{ij}(\theta)$. By contrast, if the coordinate axes are determined [12] by $\hat{\mathbf{k}}$ and $\boldsymbol{\epsilon}$ (assuming linear polarization), $\hat{\mathbf{p}}\cdot\hat{\mathbf{k}}$ and so C_{ij} will depend on both polar and azimuthal angles. The fact that the C_{ij} can be written as single-variable functions is of considerable importance for tabulation. This simplicity we achieve in the functional dependence of C_{ij} is at the expense of defining the Stokes parameters of the incoming photon relative to the chosen direction of observation of the ejected photoelectron. For discussion of these two coordinate systems, see [11–13]. Analogous to the expansion of the angular distribution shape in Legendre polynomials, the corresponding expansion for C_{23} [10,12,13] is

$$C_{23}(\omega,\theta)=S^{-1}(\omega,\theta)\sum_{l=2}^{\infty}\zeta_{2l}(\omega)L_l P_l^m(\theta), \quad (2)$$

where instead of B_l $\zeta_{2l}(\omega)$ is the corresponding spin polarization parameter [14], composed of pairs of reduced matrix elements summed over multipoles and continuum states, weighted by functions in the cosine and sine of the continuum phase shifts δ; $P_l^m(\theta)$ is an associated Legendre polynomial in which $m=2$ for C_{23} and $L_l=[(l-1)!/(l+1)!]^{1/2}$.

In our numerical calculations we used the relativistic full multipole code of Goldberg [15]. Wave functions were generated in the field of a Dirac-Slater potential in the independent-particle approximation (IPA). This model should be good at energies at which RDZ's occur. Even though it is now understood that correlation contributions can remain significant at these energies [16] for non-s states, it has been found that net electron correlation contributions are generally small at high energies due to partial cancellation of such effects [17]. We note that good agreement between experimental and theoretical IPA values for C_{10} and angular distributions in the K shell has been reported in [2].

In the next section we demonstrate the connection between the occurrence of a RDZ at ω^0 and a zero in C_{23}, by tracing the feature in C_{23} to its spin polarization parameters and finally to the RDZ matrix element itself. In the following section we show how the RDZ's result directly from the Dirac equation for any potential. We give examples of simple analytic forms of RDZ matrix elements.

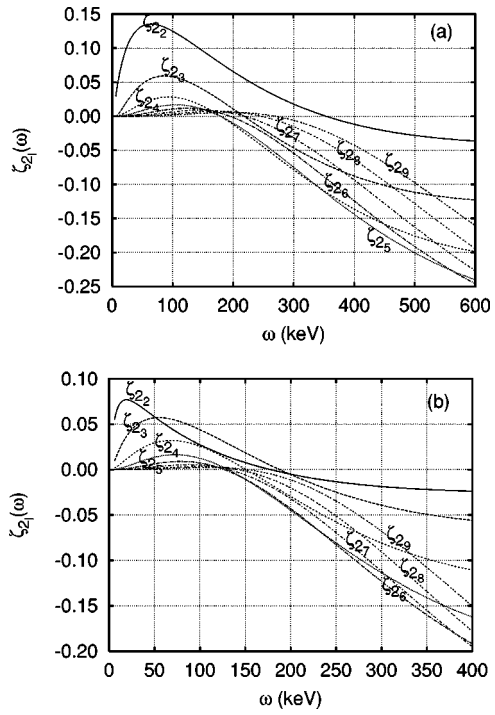

FIG. 2. The spin-polarization parameters ζ_{2l} for photoionization of neodymium ($Z=60$): (a) $4p_{3/2}$, $\omega^0=255.5$ keV; (b) $4d_{5/2}$, $\omega^0=170.3$ keV. The calculation is the same as described in Fig. 1.

II. CONNECTION BETWEEN ZEROS IN C_{23} AND RDZ MATRIX ELEMENTS

C_{23} is the only polarization correlation coefficient that consistently changes sign at an ω close to ω^0 (as l_b increases); see Fig. 1. Although C_{23} contributes to the differential cross section at order αZ, it becomes quite sizable for intermediate- to high-Z elements at photon energies on the order of hundreds of keV. However, it vanishes in the nonrelativistic and extreme relativistic limits [10,11]. We mainly use Nd (neodymium, $Z=60$) photoionization in this article to illustrate the effects of RDZ's. In Fig. 1(a) we see no sign changes in C_{23} near $\omega^0=mc^2=511$ keV for $4s_{1/2}$ photoionization, while we do see zeros for $4p_{3/2}$, $4d_{5/2}$, and $4f_{7/2}$, increasingly closer to the corresponding ω^0. In Fig. 1(b) the zero in C_{23} for $4p_{3/2}$ is near 210 keV compared to $\omega^0=mc^2/2=255.5$ keV; the zero in the case of $4d_{5/2}$ [Fig. 1(c)] is at approximately 150 keV, close to $\omega^0=mc^2/3=170.3$ keV; Fig. 1(d) shows a zero near 120 keV, very close to $\omega^0=mc^2/4=127.75$ keV, for $4f_{7/2}$. Similar results are obtained for other choices of n and Z. This trend with l_b can be expected, because, for smaller l_b, ω^0 is larger and is now at energies at which higher multipole contributions become more important. As one can see from Fig. 1, at these energies the relative contribution of C_{23} to $d\sigma/d\Omega$ is in the range of 2–5 % (C_{23} is on a scale of unity) for photoelectron ejection angles between 20° and 50°. [The positions of zeros in C_{23} deviate from ω^0 for $\theta>50°$, due to sign changes in the $P_l^2(\theta)$ that alter the near-cancellation of corresponding $\zeta_{2l}L_lP_l^2$ terms which occurs at smaller angles, and so they no longer provide a signature for the RDZ matrix elements.]

Whenever $l_b>0$, the ζ_{2l}'s always have zeros close to ω^0.

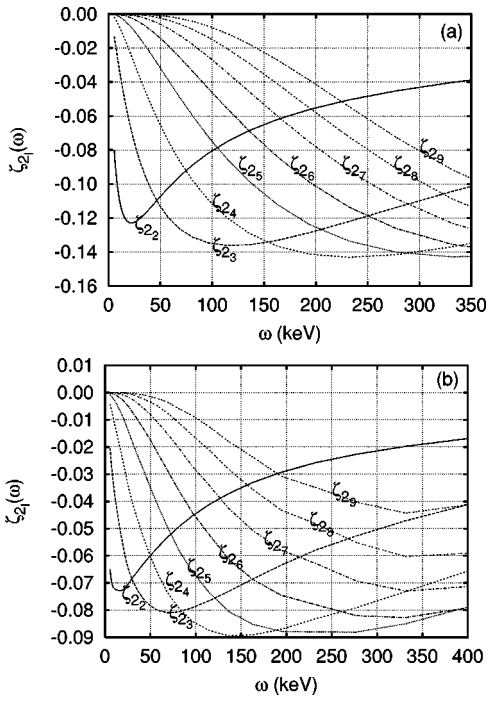

FIG. 3. Same as Fig. 2 but for (a) $4d_{3/2}$; (b) $4f_{5/2}$.

This is illustrated in Fig. 2(a), which shows the $4p_{3/2}$ case, where the ζ_{2l}'s contain the $M_{4p_{3/2}\to\epsilon d_{3/2}}$ RDZ matrix element. The zeros in ζ_{2l} become progressively closer to ω^0 with increasing l_b. This is illustrated in comparison with the results in Fig. 2(b), for $4d_{5/2}$, which contains $M_{4d_{5/2}\to\epsilon f_{5/2}}$. For $4d_{3/2}$, [Fig. 3(a)] and $4f_{5/2}$ [Fig. 3(b)], where the ζ_{2l}'s contain $M_{4d_{3/2}\to\epsilon p_{3/2}}$ and $M_{4f_{5/2}\to\epsilon d_{5/2}}$, respectively, which are non-RDZ matrix elements, no zeros result. This is also true for all other cases of $(n,l_b,j_b)\to(\epsilon,l_b-1,j_b)$ matrix elements.

We now assess the relative importance of RDZ matrix elements in C_{23} by partitioning its components, corresponding to the components of SC_{23} [the numerator of Eq. (2)], into two groups, one (C_{RDZ}) consisting of all terms that include RDZ matrix elements and one (C_{oth}) containing all other terms. In the cases of $4p_{3/2}$, $4d_{5/2}$, and $4f_{7/2}$ [Figs. 4(a), 4(b), and 4(c), respectively], C_{RDZ} is dominant for ω up to about 100 keV and it is largely responsible for the positive value of C_{23} at low energies. C_{RDZ} and C_{oth} do display some Z dependence, which is apparent in comparing Fig. 4 with Figs. 5(a), 5(b), and 5(c) when $Z=92$. However, the general behavior is similar at all Z. Dependence on the primary quantum number n is generally very small. C_{oth} is generally small (sometimes becoming negative for higher Z) over a broad energy range, reflecting partial cancellation among its terms as they individually begin to increase in size. In all cases C_{RDZ} is sufficiently dominant to prevent any sign change in C_{23} at lower energies and to cause a zero in C_{23} close to ω^0. It should be noted that C_{23} vanishes at both forward and backward angles; it tends to be largest at angles between about 20° and 50°. The effects of RDZ's in $d\sigma/d\Omega$ may best be observed over this range of angles, for energies ranging from 100 to about 300 keV.

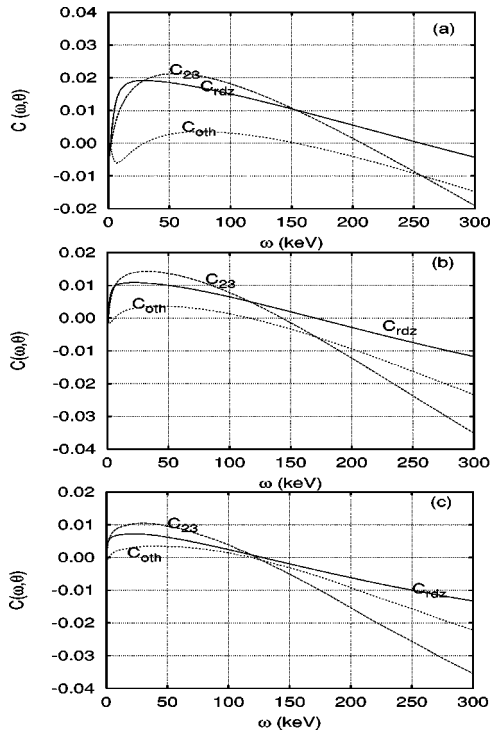

FIG. 4. C_{RDZ} represents all terms in C_{23} for which SC_{23} contains a RDZ matrix element. All remaining terms are contained in $C_{\mathrm{oth}}=C_{23}-C_{\mathrm{RDZ}}$. $C_{\mathrm{RDZ}}=(\Sigma_{\lambda\kappa_c}M^{1}_{\kappa_c',\kappa_b}M^{\lambda}_{\kappa_c\kappa_b})/S$. $M_{\kappa_c\kappa_b}$ contain the matrix elements of multipolarity λ phase shifts and the vector coupling coefficients as described in [10]. Here $Z=60$ and $n=4$. The calculation is the same as described in Fig. 1, for the case $\theta=25°$. (a) $4p_{3/2}$, $\omega^0=255.5$ keV, $\kappa_b=-2$ $(p_{3/2})$, $\kappa_c'=2$ $(d_{3/2})$; (b) $4d_{5/2}$, $\omega^0=170.3$ keV; $\kappa_b=-3$ $(d_{5/2})$, $\kappa_c'=3$ $(f_{5/2})$; (c) $4f_{7/2}$, $\omega^0=127.75$ keV, $\kappa_b=-4$ $(f_{7/2})$, $\kappa_c'=4$ $(g_{7/2})$.

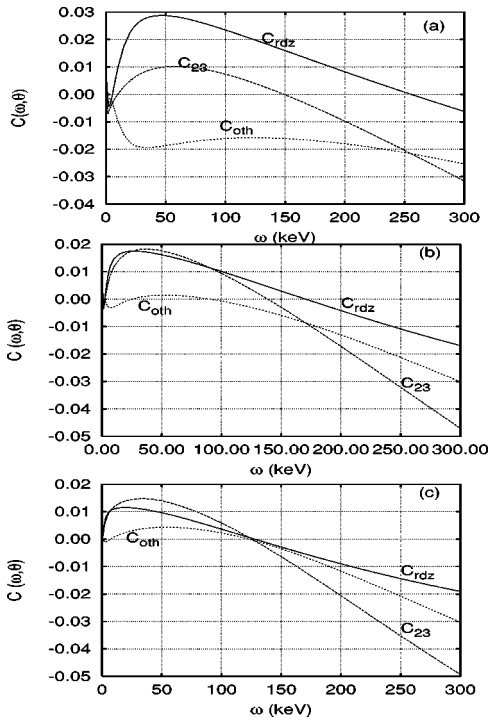

FIG. 5. Same as Fig. 4 but for $Z=92$.

III. PROPERTIES OF RDZ MATRIX ELEMENTS: GENERAL PROOF OF ZEROS AND EXPLICIT ANALYTIC EXPRESSIONS

Now that we have established a link between zeros in C_{23} and the RDZ matrix element, we try to explain how and why RDZ's occur. We first give a proof that RDZ exists at $\omega^0=mc^2/(l_b+1)$ when $\kappa_b+\kappa_c=0$ for any n, Z, and potential V. We then obtain explicit expressions for RDZ matrix elements under simplifying assumptions and see how they explicitly exhibit the zeros.

For our proof we use the following two sets of commutators:

$$H_{\kappa_c}[-i\alpha_r j_{l-1}(\rho)]=[-i\alpha_r j_{l-1}(\rho)]H_{\kappa_b}-k\frac{dj_{l-1}(\rho)}{d\rho}+\frac{\beta j_{l-1}(\rho)(\kappa_c+\kappa_b)}{r}+2i\alpha_r\beta j_{l-1}(\rho), \tag{3}$$

$$H_{\kappa_c}\left(\frac{dj_{l-1}(\rho)}{d\rho}\right)=\left(\frac{dj_{l-1}(\rho)}{d\rho}\right)H_{\kappa_b}-i\alpha_r k\left(\frac{d^2j_{l-1}(\rho)}{d\rho^2}\right)-\frac{i\alpha_r\beta(\kappa_c-\kappa_b)}{\rho}\left(\frac{dj_{l-1}(\rho)}{d\rho}\right), \tag{4}$$

where j_l is a spherical Bessel function, α_r and β are radial Dirac matrices, $\rho=kr$, k is the photon momentum, ϵ,E_b are the electron kinetic and bound-state energies corresponding to the κ_c and κ_b states, and H_κ is the radial Dirac Hamiltonian [see [18], Eq. (53.11)]. We take expectation values of the operator Eqs. (3) and (4) between bound and continuum radial states. We utilize the fact that the Dirac Hamiltonian is Hermitian, $H_{\kappa_c}\psi_{\kappa_c}=\epsilon\psi_{\kappa_c}$ and $H_{\kappa_b}\psi_{\kappa_b}=E_b\psi_{\kappa_b}$, with $k=\epsilon-E_b$, and we require the condition $\kappa_b+\kappa_c=0$. Then subtraction of the expectation values of Eq. (4) from those of Eq. (3), and utilizing identities for the derivatives of spherical Bessel functions [[19], Eqs. (11.162) and (11.171)], yields

$$-\left(\frac{2k}{3}\right)\langle i\alpha_r[j_0(\rho)+j_2(\rho)]\rangle+2\left\langle i\alpha_r\beta\left[\frac{k\kappa_c}{3}[j_0(\rho)+j_2(\rho)]-j_0(\rho)\right]\right\rangle=0. \tag{5}$$

The electric-field dipole matrix element when $\kappa_b+\kappa_c=0$ [[20], Eq. (11a)] is

$$M=-2\kappa_c\left\langle i\alpha_r\beta\left(j_0(\rho)-\frac{1}{3}[j_0(\rho)+j_2(\rho)]\right)\right\rangle-\frac{2}{3}\langle i\alpha_r[j_0(\rho)+j_2(\rho)]\rangle. \tag{6}$$

Subtracting Eq. (5) from Eq. (6) yields

$$M=\frac{2}{3k}(1-k\kappa_c)\langle i\alpha_r j_0(\rho)\rangle, \tag{7}$$

which confirms that, whenever $\kappa_b+\kappa_c=0$ with $\kappa_b<0$, $M=0$ when $k=\omega_0=mc^2/\kappa_c=mc^2/(l_b+1)$ ($k=\omega$ in our dimensionless units with $m=\hbar=c=1$). Note in the nonrelativistic limit of Eq. (7), when $\omega \ll mc^2$, $1-k\kappa_c \to 1$ and the zero no longer occurs.

We now illustrate RDZ behavior in explicit analytic calculations of the matrix elements. The result for ω^0 was independent of the potential V, so we use the Coulomb potential, which in fact is quite accurate for matrix elements at these energies (except for normalization). Since one can show that the result for ω^0 is also independent of retardation (for these energies retarded and nonretarded dipole matrix elements only differ by 10–20%), we consider the nonretarded case [i.e., $j_0=1$, $j_l=0$ if $l>1$; see Eq. (6)] when $\kappa_b+\kappa_c=0$. Using the Coulombic radial wave functions [21,22], we integrate over r by a Laplace transform [[23], Eq. (7.621)] and follow with a Kumar transformation [[23], Eq. (9.31)], which yields a terminating series for the resulting hypergeometric function, and we obtain

$$M=(2/3)\left[(2\kappa_c-1)\int gFr^2dr+(2\kappa_c+1)\int fGr^2dr\right]$$
$$=-A_{n'}[(2\kappa_c-1)U^+\,\mathrm{Im}(B^+_{n'})$$
$$+(2\kappa_c+1)U^-\,\mathrm{Re}(B^-_{n'})]. \qquad (8)$$

This equation only applies to $l_b \to l_b \pm 1$ transitions when $\kappa_b+\kappa_c=0$. (G,g) and (F,f) are the large and small components of the bound (upper case) and continuum (lower case) radial wave functions, respectively. $A_{n'}$, $B^{\pm}_{n'}$, and $U^{\pm}$ are given in the Appendix.

In Eq. (8) one finds that $\int fGr^2dr$ always has a zero at $2mc^2$ and $\int gFr^2dr$ one at $-2mc^2$. In the nodeless case ($n'=0$) Eq. (8) becomes

$$M=-Q_0A_0[(2\kappa_c-1)(\omega+2)+(2\kappa_c+1)(\omega-2)]$$
$$=4Q_0A_0(1-\kappa_c\omega), \qquad (9)$$

where $Q_0=(2\omega)^{1/2}\kappa_c(\alpha Z)$, showing the zeros in the two radial integrals (first equation) and showing ω^0 as the position of the RDZ (second equation). Note that κ_c in the polynomial $(1-\kappa_c\omega)$ which determines ω^0 comes from the radial integral coefficients $2\kappa\pm1$ shown in Eq. (8). Equation (9) can be generalized for any n' (i.e., $A_0 \to A_{n'}$ and $Q_0 \to Q_{n'}$) due to the relationship $\int gFr^2dr/\int fGr^2dr=(\omega+2)/(\omega-2)$, an identity that can be established as generally valid by considering $\int(d/dr)(gG+fF)r^2dr=0$ and applying the Dirac equation. Here $Q_{n'}$ can involve polynomials in ω. As a consequence, the square brackets in Eq. (9) (first equation) and the quantity $(1-\kappa_c\omega)$ (second equation), as well as the result $\omega^0=mc^2/(l_b+1)$, are general, independent of n and V, and arise from the energy, κ, and mc^2 terms in the Dirac equation [[18], Eq. (53.15)]. Note that there is no zero in $(1-\kappa_c\omega)$ for $l_b \to l_b-1$ transitions, in which κ_c is negative, so that $(1-\kappa_c\omega)$ can only vanish for negative ω.

We can confirm the relativistic character of the RDZ's by considering the nonrelativistic limit of M [Eq. (8)]. If we take a partial limit, letting $\gamma=|\kappa|$, but not otherwise dropping terms of order $(\alpha Z)^2$, the position of the zeros becomes dependent on n and Z. If we complete taking the nonrelativistic limit by dropping the remaining $(\alpha Z)^2$ consistently and introducing the low-energy approximation $(\omega \pm mc^2 \approx \pm mc^2)$, we can show both numerically and analytically that there are no photoionization zeros in M. Numerical examples for $Z=92$ which illustrate this behavior are shown in Fig. 6 for $M_{1s_{1/2}\to\epsilon p_{1/2}}$ and $M_{4d_{5/2}\to\epsilon f_{5/2}}$. In general, when γ is replaced by $|\kappa|$ the deviation in the matrix element from ω^0 increases with increasing Z but decreases with increasing n. Both graphs show that the zeros disappear in the nonrelativistic limit. The disappearance of RDZ's is illustrated in the analytic RDZ matrix-element expression for $n'=0$, which in the nonrelativistic limit M^{nrl} becomes

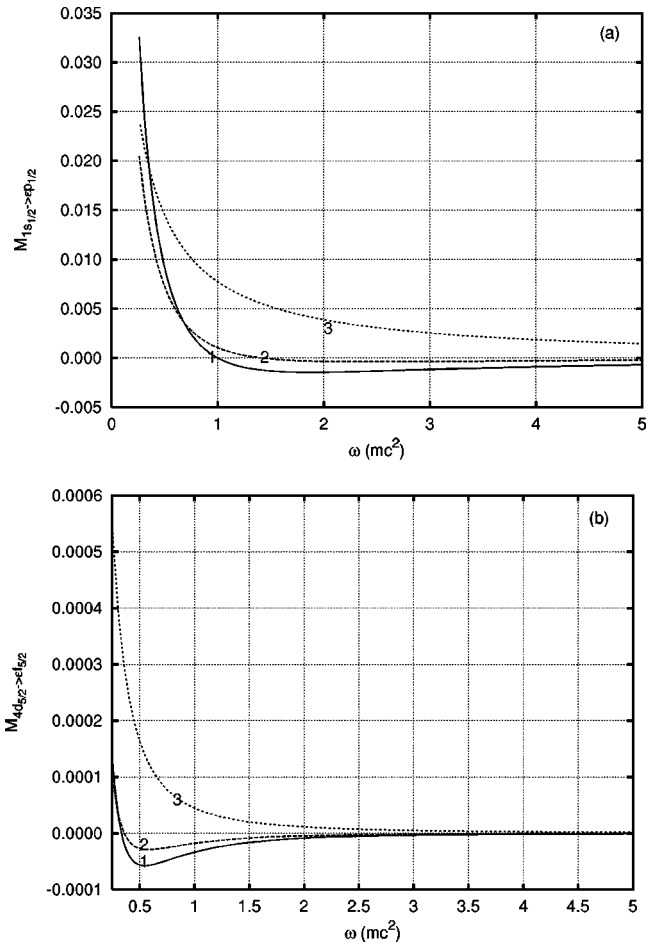

FIG. 6. (a) Dipole nonretarded matrix element $M_{1s_{1/2}\to\epsilon p_{1/2}}$ for $Z=92$; (1) relativistic; (2) γ replaced by $|\kappa|$; (3) nonrelativistic limit. (b) Same as (a) but for $M_{4d_{5/2}\to\epsilon f_{5/2}}$.

$$M^{\mathrm{nrl}}=4A_0^{\mathrm{nrl}}(\kappa_c^2+q^2)^{1/2}(n-\kappa_b)(2\omega)^{1/2}\kappa_c\alpha Z, \qquad (10)$$

where q is defined in the Appendix. A_0^{nrl} is the nonrelativistic limit of A_0. There are no terms in Eq. (10) that can change sign with any change in energy. Similar expressions, though more complicated, can also be obtained for $n'>0$, again reflecting the absence of any photoionization zeros.

IV. CONCLUSIONS

We have shown that RDZ's are a special class of zeros whose positions ω^0 depend only on l_b, according to $\omega^0 = mc^2/(l_b+1)$, where ω^0 is thus independent of V and the inclusion of dipole retardation. The fact that RDZ's disappear in the nonrelativistic limit forms of their matrix elements due to their dependence on mc^2 confirms that RDZ's are relativistic. We have found these zeros for the case of Dirac relativistic dipole matrix elements; the condition for the occurrence of a zero for given l_b is that bound and continuum Dirac quantum numbers $\kappa_b+\kappa_c=0$. Finally, RDZ's have observable physical consequences, particularly for the polarization correlation C_{23}, at energies for which cross sections and spin-polarization correlations have already been measured.

APPENDIX

$$A_{n'} = DH_{\kappa_b}^{-(\gamma+1)} \exp\{-2y \tan^{-1}[N_{\kappa_b} p(\alpha Z)^{-1}]\} \times \prod_{k=1}^{n'} (2\gamma+k),$$

$$B_{n'}^{\pm} = T\left\{ J_{\kappa_b,0}^{\pm} C_{\kappa_b} + \sum_{j=1}^{n'} \frac{(-1)^j}{j!} J_{\kappa_b,j}^{\pm} (2\alpha Z)^j \left(\frac{C_{\kappa_b}^*}{H_{\kappa_b}}\right)^{j-1} \times S_j \left[1 + \sum_{m=1}^{j} \frac{(-1)^m}{m!} \left(\frac{2N_{\kappa_b} p}{iC_{\kappa_b}^*}\right)^m W_{mj} \right] \right\}.$$

Here $U^{\pm} = (w\pm 1)^{1/2}(1\mp\xi_{\kappa_b})^{1/2}$; the photoelectron energy $w=\omega-E_b+1$; $\xi_{\kappa_b} = \{1+[\alpha Z/(n'+\gamma)]^2\}^{-1/2}$; $n' = n - |\kappa_b|$; $\gamma=\gamma_b=\gamma_c=[|\kappa|^2-(\alpha Z)^2]^{1/2}$. $A_{n'}$, collecting all real terms common to both radial integrals, depends on

$$N_{\kappa_b} = [n^2 - 2n'(|\kappa_b|-\gamma)]^{1/2}; \quad H_{\kappa_b} = (\alpha Z)^2 + (N_{\kappa_b} p)^2;$$

$$y = \alpha Z w/p; \quad p = (w^2-1)^{1/2};$$

$$D = 2^{\gamma+1} 3^{-1} P^{\gamma-1/2} \exp(\pi y/2)(2\alpha Z/N_{\kappa_b})^{\gamma+1/2} |\Gamma(\gamma - iy)| / [4\pi n'! N_{\kappa_b}(N_{\kappa_b}-\kappa_b)\Gamma(2\gamma+1)]^{1/2}.$$

$B_{n'}^{\pm}$ collects all complex terms, the imaginary part corresponding to $\int gFr^2 dr$ and the real part to $\int fGr^2 dr$. In $B_{n'}^{\pm}$, $T = (\kappa_c - iq)^{1/2}(\gamma+iy)^{1/2}$; $q = y/w$; $C_{\kappa_b} = \alpha Z + iN_{\kappa_b} p$; $J_{\kappa_b j}^{\pm} = N_{\kappa_b} - \kappa_b \pm (n'-j)$; $S_j = \Pi_{l=1}^{j}(n'+1-l)$; and $W_{mj} = \Pi_{s=1}^{m}(j+1-s)(\gamma+s+iy)(2\gamma+s)^{-1}$.

[1] Y. S. Kim (private communication); X. M. Tong, L. Lei, and J. M. Li, Phys. Rev. A **49**, 4641 (1994).

[2] B. A. Logan, J. Phys. A **4**, 346 (1971); B. A. Logan, R. J. Jones, A. Ljubicic, W. R. Dixon, and R. Storey, Phys. Rev. A **10**, 532 (1974); Can. J. Phys. **53**, 1721 (1975).

[3] P. R. S. Gomes and J. Byrne, J. Phys. B **13**, 3975 (1980).

[4] U. Fano and J. W. Cooper, Rev. Mod. Phys. **40**, 441 (1968); A. Msezane and S. T. Manson, Phys. Rev. Lett. **35**, 364 (1975); **48**, 473 (1982).

[5] R. H. Pratt, R. Y. Yin, and X. Liang, Phys. Rev. A **35**, 1450 (1987).

[6] R. Y. Yin and R. H. Pratt, Phys. Rev. A **35**, 1149 (1987).

[7] M. S. Wang and R. H. Pratt, Phys. Rev. A **29**, 174 (1984).

[8] R. Y. Yin and R. H. Pratt, Phys. Rev. A **35**, 1154 (1987).

[9] M. S. Wang, Y. S. Kim, R. H. Pratt, and A. Ron, Phys. Rev. A **25**, 857 (1982).

[10] R. H. Pratt, A. Ron, and H. K. Tseng, Rev. Mod. Phys. **45**, 273 (1973).

[11] R. H. Pratt, R. D. Levee, R. L. Pexton, and W. Aron, Phys. Rev. **134**, A898 (1964); **134**, A916 (1964); Y. S. Kim, I. B. Goldberg, and R. H. Pratt, Phys. Rev. A **45**, 4542 (1992); **51**, 424 (1995).

[12] A. Derevianko, W. R. Johnson, and K. T. Cheng, At. Data Nucl. Data Tables **73**, 154 (1999).

[13] A. Bechler and R. H. Pratt, Phys. Rev. A **42**, 6400 (1990).

[14] K. N. Huang, Phys. Rev. A **26**, 3676 (1982).

[15] I. Goldberg, Internal Report No. PITT-291, 1982 (unpublished).

[16] E. W. B. Dias, H. S. Chakraborty, P. C. Deshmukh, S. T. Manson, O. Hemmers, P. Glans, D. L. Hanson, H. Wang, S. B. Whitfield, D. W. Lindle, R. Wehlitz, J. C. Levin, I. A. Sellin, and R. C. C. Perera, Phys. Rev. Lett. **78**, 4553 (1997); D. L. Hansen, O. Hemmers, H. Wang, D. W. Lindle, P. Focke, I. A. Sellin, C. Heske, H. S. Chakraborty, P. C. Deshmukh, and S. T. Manson, Phys. Rev. A **60**, R2641 (1999).

[17] V. K. Dolmatov and S. T. Manson, Phys. Rev. A **63**, 022704 (2001); V. K. Dolmatov, A. S. Baltenkov, and S. T. Manson, *ibid.* **64**, 042718 (2001).

[18] L. I. Schiff, *Quantum Mechanics* (McGraw-Hill, New York, 1968), pp. 483–484.

[19] G. Arfken, *Mathematical Methods for Physicists* (Academic, London, 1985).

[20] J. H. Scofield, Phys. Rev. A **40**, 3054 (1989).

[21] H. A. Bethe and E. E. Salpeter, *Quantum Mechanics of One and Two Electron Atoms* (Springer-Verlag, Berlin, 1957), p. 69.

[22] M. E. Rose, *Relativistic Electron Theory* (Wiley, New York, 1961), p. 194.

[23] I. S. Gradshteyn and M. Ryzhik, *Table of Integrals, Series and Products* (Academic, New York, 1980), p. 860, Eq. (4).